TEST CASE DOCUMENTATION
AND TESTING RESULTS

TEST CASE ID EM-VER-4.1

Simulation of a Railgun

Tested with LS-DYNA® v980 Revision Beta

Friday 23rd March, 2012

Document Information	
Confidentiality	**external use**
Document Identifier	LSTC-QA-LS-DYNA-EM-VER-4.1-1
Author(s)	Iñaki Çaldichoury, Pierre L' Eplattenier
Number of pages	16
Date created	Friday 23rd March, 2012
Distribution	LS-DYNA® QA and Support Department

Contents

1 Introduction

1.1 Purpose of this Document

This document specifies the test case EM-VER-4.1. It provides general test case information like name and ID as well as information to the confidentiality, status, and classification of the test case.

A detailed description of the test case is given, the purpose of the test case is defined, and the tested features are named. Results and observations are stated and discussed. Testing results are provided in section 4.1 for the therein mentioned LS-DYNA® version and platforms.

2 Test Case Information

Test Case Summary	
Confidentiality	external use
Test Case Name	Railgun: Using the LS-DYNA electromagnetic contact algorithm to simulate a railgun
Test Case ID	EM-VER-4.1
Test Case Status	active
Test Case Classification	Verification
Metadata	ACADEMIC/INDUSTRIAL TEST CASE

Table 1: Test Case Summary

3 Test Case Specification

3.1 Test Case Purpose

The purpose of this test case is to analyze the EM solver's electromagnetic contact capabilities through a complex verification test case that involves setting up an analytical model that may be later modified under some assumptions and to compare the results with those given by LS-DYNA.

3.2 Test Case Description

In its most basic form , a railgun consists of two parallel metal rails connected to an electric power supply. When a projectile is inserted between the two bars, it provides a conductive path between the rails thus completing the circuit. The current flowing through the rails and armature generates a magnetic field between the bars which, in turn, creates a Lorenz force applied on the projectile (See Figure (1)). This force will propel the projectile and then eject it from the end of the railgun at a very high speed. Based on the physical equations for this problem and on some hypothesis that will be further discussed, this section describes a simple analytical model that can be used to simulate a railgun model such as proposed by [1].

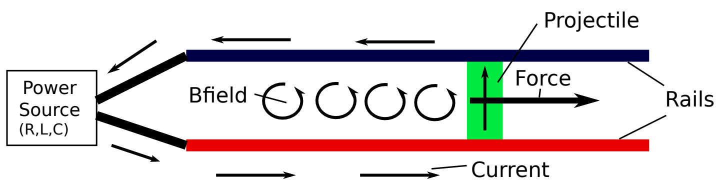

Figure 1: Schematic representation of a railgun model

The chosen system consists in a storage capacitor (R_0, L_0, C circuit) connected to the railgun bars and discharging when the railgun is ready to fire. The circuit equation gives :

$$\frac{q}{C} + \frac{dLi}{dt} + Ri = 0 \tag{1}$$

where q is the circuit charge, C the circuit capacity, L the whole circuit's inductance (Rails, projectile and power source), i the current and R the whole circuit's resistance .

The current can be expressed as a function of the charge :

$$i = \frac{dq}{dt} \tag{2}$$

The initial conditions yield :

$$q(o) = Q_0, \frac{dq(0)}{dt} = 0 \tag{3}$$

where Q_0 is the initial charge of the capacitor ($Q_0 = CU_0$ with U_0 being the initial voltage applied to the system).

Replacing (2) in (1), we get :

$$\frac{q}{C} + \frac{dL}{dt}\frac{dq}{dt} + L\frac{d^2q}{dt^2} + R\frac{dq}{dt} = 0 \tag{4}$$

with :

$$\frac{dL}{dt} = \frac{dL}{dx}\frac{dx}{dt} = V\frac{dL}{dx}. \quad (5)$$

where V is the projectile's velocity and $\frac{dL}{dx}$ is now only dependent of the geometry.

Furthermore, the Lorentz force applied on the projectile can be written such as :

$$F = M\frac{dV}{dt} = \frac{1}{2}i^2\frac{dL}{dx} \quad (6)$$

with M being the mass of the solid.

In order to solve equation (4) and (6), a representation of the Resistance's and inductance's behavior as a function of the projectile's displacement x are needed. The circuit's resistance can be computed as :

$$R = R_0 + 2R_{rail} + R_{projectile} = R_0 + 2\frac{x}{\sigma_{rail}S_{rail}} + \frac{L_{projectile}}{\sigma_{projectile}S_{projectile}} \quad (7)$$

where R_0 is the initial resistance of the power source (R_0, L_0, C circuit), σ, the material's conductivity, $L_{projectile}$ the size of the projectile (See Figure (2)).

The behavior of the inductance of the rail gun system is not known. A first approach would be to use the expression of the external inductance for parallel plane transmission lines. According to this model, the inductance of the rail gun follows the following behavior :

$$L = L_0 + \mu_0\frac{L_{projectile}}{Rw}x \quad (8)$$

where L_0 would be the initial inductance of the power source (R_0, L_0, C circuit),μ_0 the permeability of free space and Rw, the railgun width (See Fig. 2).

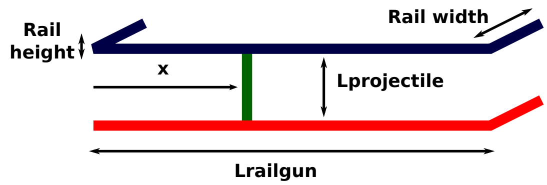

Figure 2: Geometry of the railgun model

For the railgun system that was designed the parameter set and the geometric considerations are inspired by [1] and are listed in Table (2) and (3).

Figure (3) and Figure (4) give the results of the previously described analytical model for the displacement of the projectile, its final velocity, the behavior of the system's current, charge, inductance and resistance as well as the associated energies. The results obtained are similar to those of [1]. However, this model was based on two simplifying hypothesis that may be

Circuit parameters	
U_0	400 (Volts)
R_0	0 (Ohm)
C	2.02 (Faradays)
σ_{rail}	4.4e6 (S.I)
$\sigma_{projectile}$	4.4e6 (S.I)

Table 2: Circuit parameters

Railgun Geometry	
$L_{railgun}$	1 (Meters)
$L_{projectile}$	30e-3 (Meters)
$Rail_{width}$	30e-3 (Meters)
$Rail_{height}$	10e-3 (Meters)
$Projectile_{width}$	20e-3 (Meters)

Table 3: Railgun Geometry

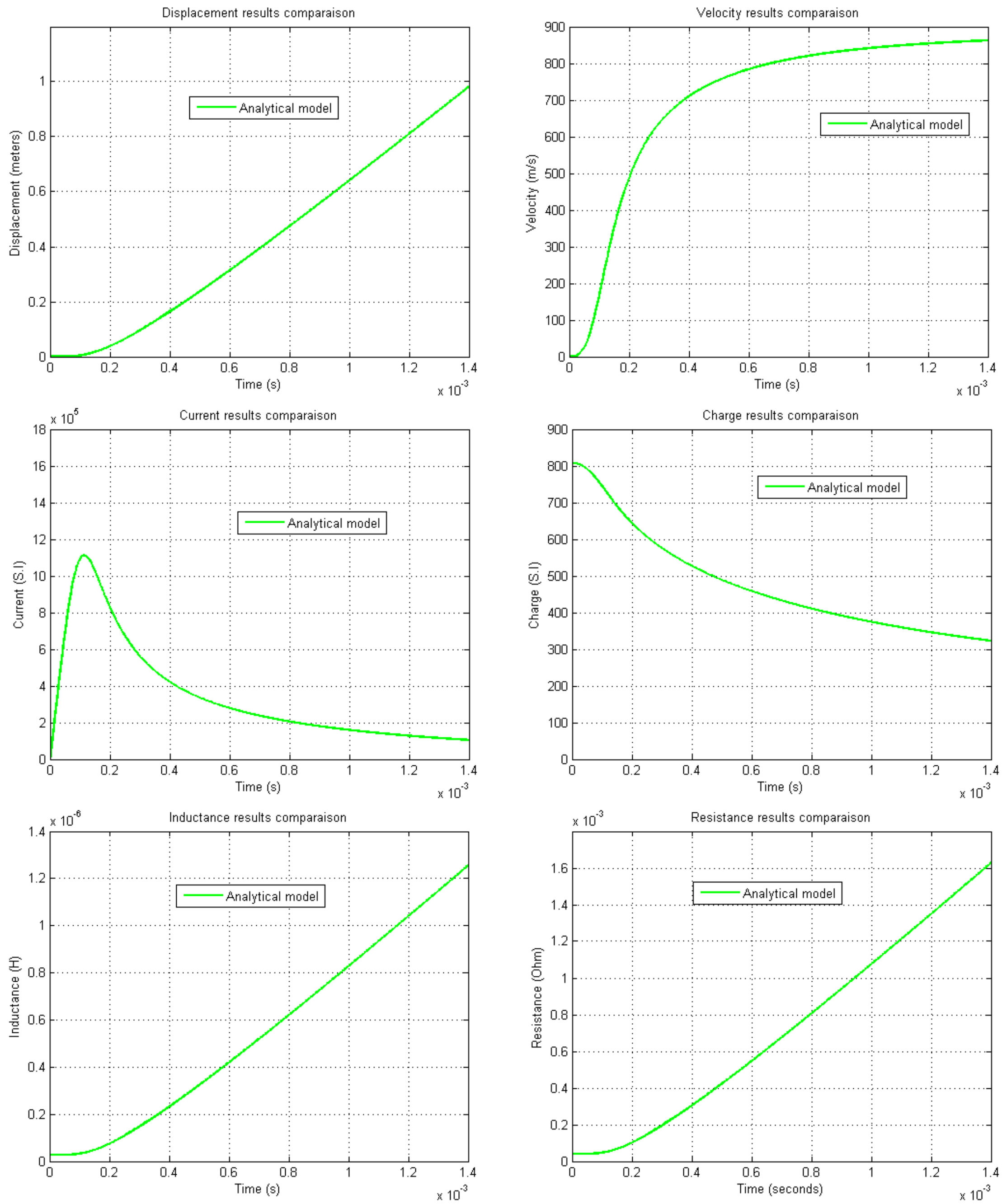

Figure 3: Railgun variables during firing given by the analytical model

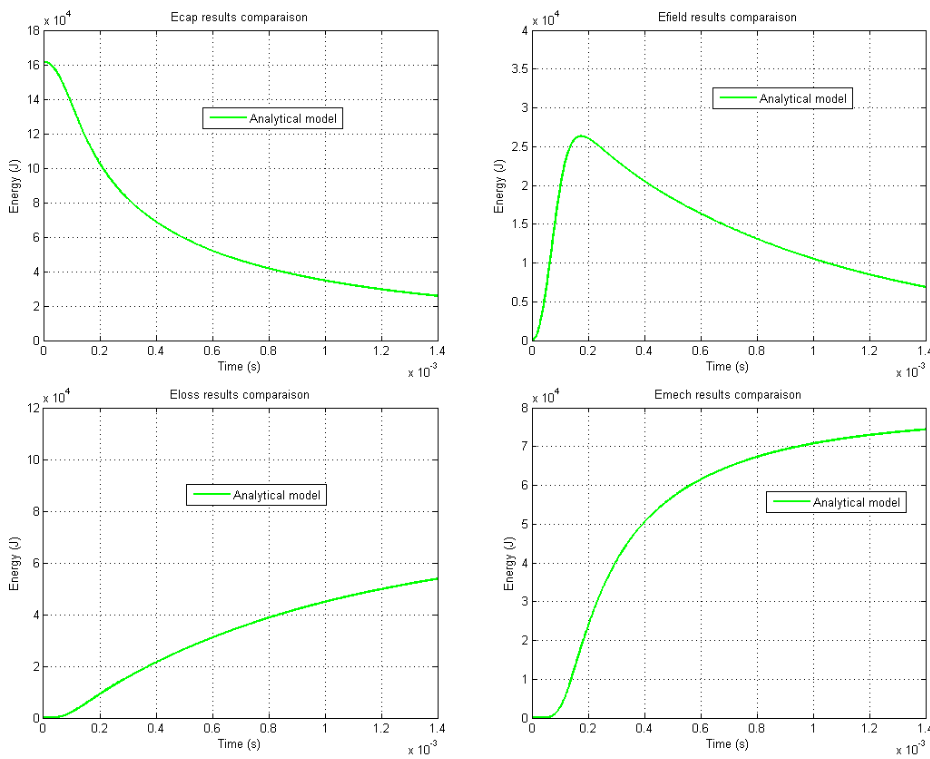

Figure 4: Railgun Energy variables during firing given by the analytical model

discussed. First of all, the propagation of the current is not entirely homogeneous which could change the slope of the Resistance function. Secondly, the most violent hypothesis is certainly the fact that the expression of the external inductance for parallel plane transmission lines has been used to estimate the behavior of the inductance. This would imply infinite rails for the railgun which in practice can never be the case. LS-DYNA through its electromagnetism model permits the simulation of railgun models. The behavior should prove to be more accurate as LS-DYNA provides an actual measurement of the resistance and inductance of a given circuit. The objective of this test case will be to compare the results given by LS-DYNA with those of the analytical model and to verify them with a corrected analytical model that will use LS-DYNA's inductance and resistance values and implement them in place of the former hypotheses.

3.3 Model Description

The electromagnetism contact algorithm creates internally a BEM mesh that connects with the closest nodes and elements of the two parts that come in contact. This BEM mesh is recomputed when its distortion is too great using a new set of nodes and elements of the two parts that remain in contact. Therefore, in order to avoid errors, one should use a fine mesh in the direction of the moving part i.e in the rail direction in this test case. As can be seen on Figure (5) a finer mesh is used in areas where, according to the analytical model, the current will reach its peak so as to retain a good precision of the results. Figure (6) and Table (4) give some information about the location of these finer zones and about their element size. All dimensions are given in millimeters. The parameters chosen for this test case reproduce those of the analytical case.

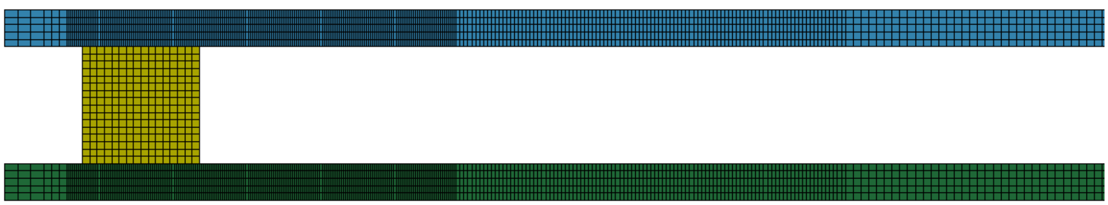

Figure 5: Test case Mesh

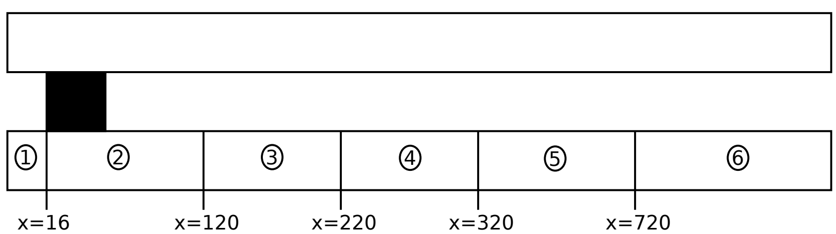

Figure 6: Test case Meshing zones (Locations given in millimeters)

Model information	
Elements size, Zone 1 (x-direction)	2
Elements size, Zone 2 (x-direction)	0.5
Elements size, Zone 3 (x-direction)	1
Elements size, Zone 4 (x-direction)	2
Elements size, Zone 5 (x-direction)	4
Elements size, Zone 6 (x-direction)	9.5
Elements size, Projectile	1.875
Total number of Nodes	104737
Total number of Elements	81856

Table 4: Test Case Mesh information

4 Test Case Results

4.1 Test Case observations

The magnetic field generated by the circuit behind the projectile that generated the force expelling it can be seen on Figure (7). Figure (8) offers a view of the current density at two different times, when the projectile reaches the very fine mesh defined as zone 2 and when it reaches the coarse mesh defined as zone 6. When the projectile crosses zone 2, a very small gap where the current density is null (blue color) between the projectile base and the rail can be observed. This is due to the BEM mesh that "occults" the closest elements of the rail in contact with the projectile. When the projectile crosses the coarser mesh of zone 6, this gap where no current diffusion is calculated logically grows. However, by the time the projectile reaches this zone, the railgun is almost entirely discharged and it is believed that the influence on the results of this coarser mesh can be neglected.

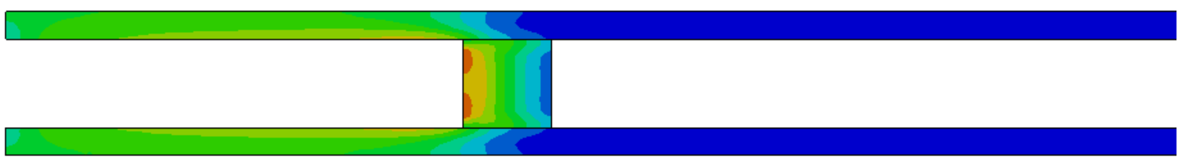

Figure 7: Test Case Magnetic field

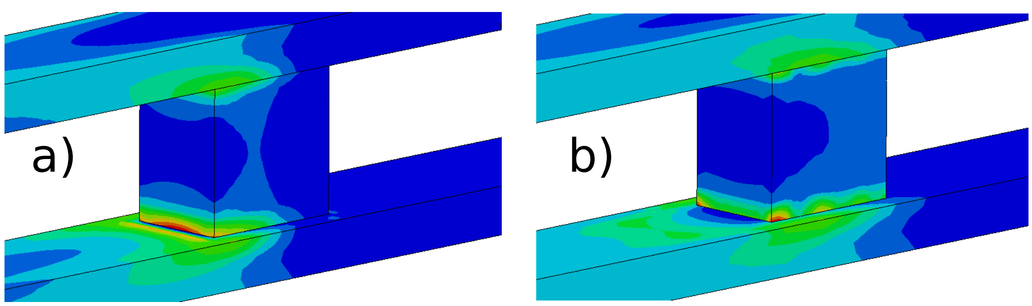

Figure 8: Test Case Current Density when a) projectile crossing zone 2 and b) when projectile crossing zone 6

Figure (9) and Figure (10) offer a comparison between the variable results of the analytical model and the inductance model. As can be seen on the curves showing the resistance and the inductance function of time, the first analytical hypothesis made on the resistance behavior proves to be accurate enough while the assumption made for the inductance proves to be rather diverging with the results obtained. This causes an important underestimation of the current peak while overestimating the velocity at which the projectile is expelled. Surprisingly enough, the displacement curve shows that the projectile gets expelled at about the same time for both cases. Similar conclusions can be reached when looking at the energies.

Finally, in order to verify that the electromagnetism contact algorithm yields coherent results, the resistance and inductance curves calculated by LS-DYNA have been implemented in the analytical model in place of the former assumption resulting in a a "corrected model". Figure (9) and Figure (10) show a comparison of the results. It can be observed that the results given by LS-DYNA are coherent with those given by the corrected model with a global behavior retained and a good error appreciation regarding the current peak and the final velocity of the projectile (See Table (5)). However, some overestimations of the energy losses and kinetic energy can also be observed. This discrepancies will be the object of further investigations for LS-DYNA's electromagnetic contact algorithm.

Railgun Simulation results			
	Analytical	LS-DYNA	Corrected
Displacement (Meters)	0.9815	0.9483	0.9256
Final Velocity (m/s)	862	805	775
Current peak (kA)	1120	1722	1746
Final charge (F)	324	175	175

Table 5: Results for analytical, LS-DYNA and corrected analytical models

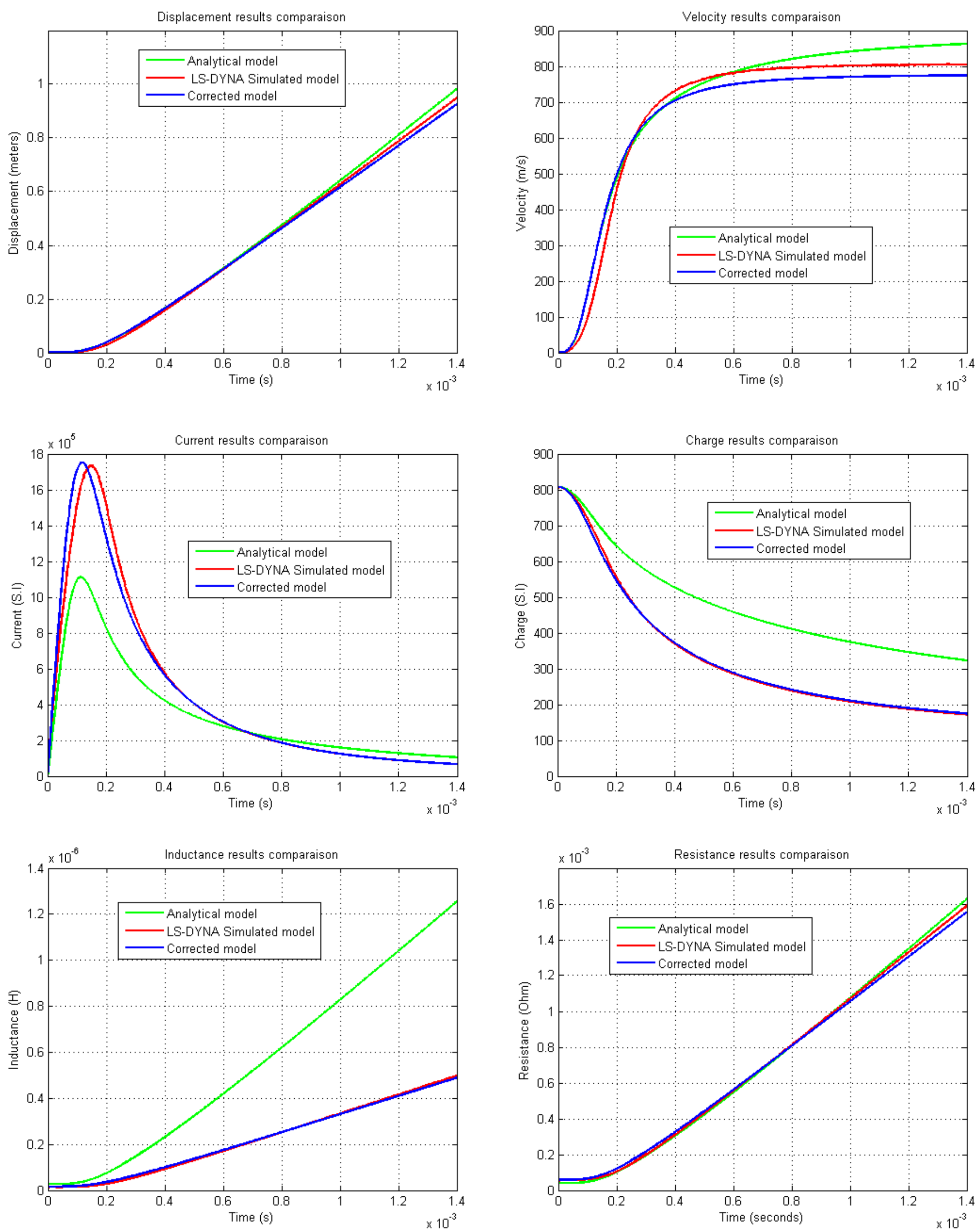

Figure 9: Comparison of variables between the analytical model, the results given by LS-DYNA and the corrected analytical model

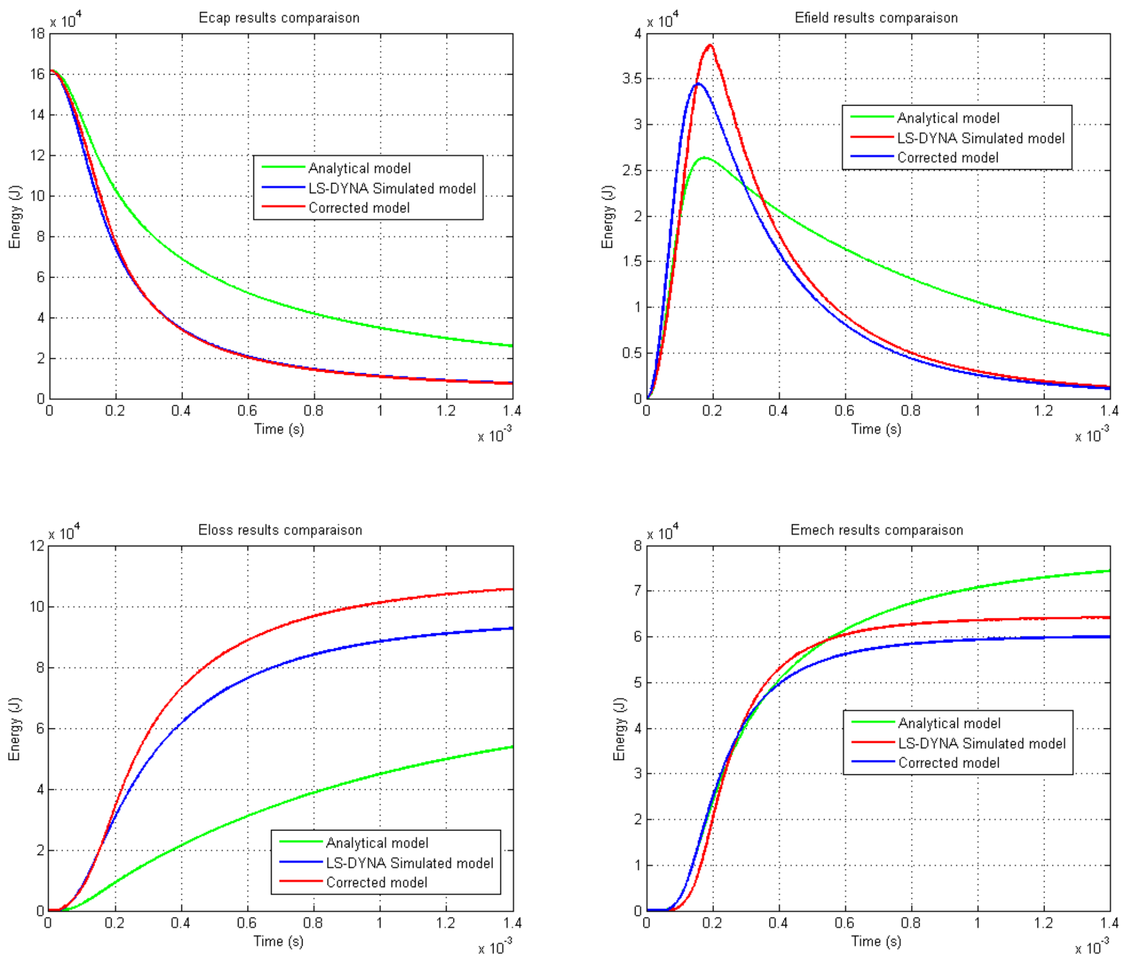

Figure 10: Comparison of energy variables between the analytical model, the results given by LS-DYNA and the corrected analytical model

References

[1] S. S. Brian Kuhn, *Pulsed power system with railgun model*, National Naval Responsibility for Naval Engineers: Education and Research for the Electric Naval Engineer.